Reynolds ridge which will provide even more insight into the unique nature of this flow. But so far it has been determined that it is the boundary condition of the surface tension gradient at the free surface in the vicinity of a Reynolds ridge which causes the flow to dynamically conform, with a rapid deceleration over a small region, resulting in a large vorticity flux at the free surface.

Acknowledgments

We would like to thank Dana Dabiri for his help and advice while performing this work. This work was supported by ONR contract# N00014-94-1-0596. The National Science Foundation, and the Zonta International Amelia Earhart Fellowship Award have supported first author Amy Warncke towards her graduate work.

References

Gharib, M., 1992, "On Some Aspects of Near Surface Vortices,"

Gharib, M., and A. Weigand, 1995, "Experimental Studies of Vortex Disconnection and Connection at a Free Surface," submitted to *Journal of Fluid Mechanics.*

Harper, J. F. and Dixon, J. N., 1974, "The Leading edge of a Surface Film on Contaminated Flowing Water," *Proc. 5th Australian Conf. on Hydraulics and Fluid Mech.,* Christchurch, New Zealand, pp. 499–505.

Lugt, H. J., 1987, "Local Flow Properties at a Viscous Free Surface," *Physics of Fluids,* vol. 30, pp. 3647–3652.

Lugt, H. J., 1988, "Fundamental Viscous Flow Properties at a Free Surface," *Fluid Dynamics Transactions,* vol. 14, pp. 1–20.

Lundgren, T. S., 1988, "A Free Surface Vortex Method with Weak Viscous Effects," Mathematical Aspects of Vortex Dynamics," *Proceedings of the Workshop on Mathematical Aspects of Vortex Dynamics,* Leesburg, VA, pp. 68–79.

Rood, E. P., 1995, "Free-Surface Vorticity," Chapter 17 in *Fluid Vortices,* S. Green, ed., Kluwer Academic Publishing, Norwell, MA.

Roesgen, T., "Dynamic Surface Slope Measurements Using Microlens Arrays," to be published in *Experiment of Fluids.*

Sellin, R. H. J., 1968, *Nature,* Vol. 217, pp. 536–538.

Scott, S. C., 1982, "Flow Beneath a Stagnant Film on Water: the Reynolds ridge," *Journal of Fluid Mechanics,* vol. 116, pp. 283–296.

Willert, C., and M. Gharib, 1991, "Digital Particle Image Velocimetry," *Experiment in Fluids,* Vol. 10, pp. 181–183.

A Novel Pump for MEMS Applications

Mihir Sen,[1] Daniel Wajerski,[1] and Mohamed Gad-el-Hak[1]

We present a novel approach for pumping fluids in micromechanical applications at extremely low Reynolds numbers. It is based on the rotation of a cylinder placed asymmetrically in a narrow duct; the differential viscous resistance between the small and large gaps causes a net flow along the channel. We report on experiments using glycerin and several cm-scale prisms having circular, square, and rectangular cross-sections. The Reynolds number, based on cylinder size and angular velocity, varies in the range of 0.01–10. The flow is visualized using tracer particles. The flow generated depends on the geometrical parameters, but is proportional to the angular velocity of the cylinder. An average flow velocity that is about ten percent of the surface speed of the cylinder has been obtained.

Manufacturing processes that can create extremely small machines have been developed in recent years. Motors, electrostatic actuators, pneumatic actuators, valves, gears, and tweezers of about 10 μm size have been fabricated. These have been used as sensors for pressure, temperature, velocity, mass flow, or sound, and as actuators for linear and angular motions. Current usage ranges from airbags to blood analysis (O'Connor, 1992). There is considerable work under way to include other applications, one example being the micro-steam engine described by Lipkin (1993). Many of these new applications will need fluid to be pumped in a duct; at such small scales this is a challenge.

There have been several studies of microfabricated pumps. Some of them use nonmechanical effects. Ion-drag is used in electrohydrodynamic pumps (Bart et al., 1990; Richter et al., 1991; Fuhr et al., 1992); these rely on the electrical properties of the fluid and are thus not suitable for many applications. Valveless pumping by ultrasound has also been proposed (Moroney et al., 1991), but produces very little pressure difference.

It is important to emphasize that mechanical pumps based on conventional centrifugal or axial turbomachinery will not work at micromachine scales where the Reynolds numbers are typically small. Centrifugal forces are negligible and, furthermore, the Kutta condition through which lift is normally generated is invalid when inertial forces are vanishingly small. In general there are three ways in which mechanical micropumps can work:

(a) Positive-Displacement Pumps. These are mechanical pumps with a membrane or diaphragm actuated in a reciprocating mode and with unidirectional inlet and outlet valves. They work on the same physical principle as their larger cousins. Micropumps with piezoelectric actuators have been fabricated (Van Lintel et al., 1988; Esashi et al., 1989; Smits, 1990). Other actuators, such as thermopneumatic, electrostatic, electromagnetic or bimetallic, can be used. These exceedingly minute positive-displacement pumps require even smaller valves, seals and mechanisms, a not-too-trivial micromanufacturing challenge. In addition, there are long-term problems associated with wear or clogging and consequent leaking around valves. The pumping capacity of these pumps is also limited by the small displacement and frequency involved. Gear pumps are a different kind of positive-displacement device.

(b) Continuous, Parallel-Axis Rotary Pumps. A screw-type, three-dimensional device for low Reynolds numbers was proposed by Taylor (1972) for propulsion purposes and shown in his seminal film. It has an axis of rotation parallel to the flow direction implying that the powering motor must be submerged in the flow, the flow turned through an angle, or that complicated gearing would be needed.

(c) Continuous, Transverse-Axis Rotary Pumps. This is the class of machines that we propose here. We assert that a rotating body, asymmetrically placed within a duct, will produce a net flow due to viscous action. The axis of rotation can be perpendicular to the flow direction and the cylinder can thus be easily powered from outside a duct. A related viscous-flow pump was designed by Odell and Kovasznay (1971) for a water channel with density stratification. However, their design operates at a much higher Reynolds number and is too complicated for microfabrication.

Fluid flow at the micromachine level is complicated by issues such as interfacial forces, slip-flow and Knudsen number effects. To develop an operational viscous-flow micropump one must first demonstrate its working at the macroscale where these special effects are not important. Our purpose here is to show experimentally that viscous forces can indeed be used to pump fluid at low Reynolds numbers. Reynolds numbers representative of micromachine applications in air or water can be obtained with cm-size cylinders and with glycerin as the working

[1] Professor, Research Assistant, and Professor, respectively, Department of Aerospace and Mechanical Engineering, University of Notre Dame, Notre Dame, IN 46556. Professor Sen is a Mem. ASME; Professor Gad-el-Hak is a Fellow ASME.

Contributed by the Fluids Engineering Division of THE AMERICAN SOCIETY OF MECHANICAL ENGINEERS. Manuscript received by the Fluids Engineering Division February 26, 1996; revised manuscript received April 24, 1996. Associate Technical Editor: D. P. Telionis.

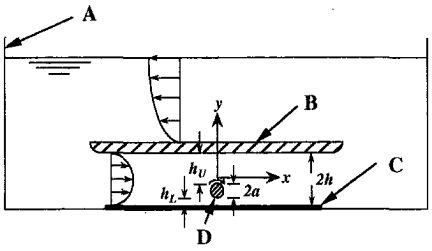

Fig. 1 Schematic of set-up

fluid. Few experiments and many numerical studies of both steady (Ingham and Tang, 1990; Tang and Ingham, 1991; Kimura et al., 1992) and unsteady (Badr et al., 1989; 1990) flow around a rotating circular cylinder are available in the open literature. There has also been work on flow around a square cylinder that is either forced to rotate (Ohba and Kuroda, 1993) or is autorotating (Zaki et al., 1994). However, there is nothing reported on the generation of a flow by rotating a cylinder.

The present laboratory experiments are carried out on the set-up shown schematically in Fig. 1. The interior dimensions of the Plexiglas tank **A** are 48.9 cm length, 15.2 cm width and 14.3 cm depth. A tightly-fitted 15.2 cm square plate **B** of the same material can be moved to any height within the tank. We are interested in the flow within the channel formed by this wall and the floor of the tank. For some of the runs a plastic sheet **C** was laid on the floor to reduce the lower gap h_L. A two-dimensional, stainless-steel cylinder **D** is placed in leak-proof bearings and can be rotated by an external electric motor (not shown). Cylinders of circular (0.898 cm diameter), square (0.898 cm diagonal) and rectangular (0.898 cm × 0.1 cm) cross-sections are tested; unless otherwise mentioned, a circular cylinder is assumed. The tank is filled with glycerin, the relative density and viscosity of which are measured before each run using a Fisher Scientific hydrometer and a Brookfield Synchro-Lectric viscometer, respectively. Due to absorption of atmospheric moisture the viscosity of the glycerin decreased from about 1.1 kg/m.s to just about one-half this value over the period of the experimentation, while the density remained approximately constant at 1260 kg/m^3. Visualization is by means of tracer particles in the fluid illuminated by a sheet of light in the mid-spanwise plane. Each run is videotaped for later analysis.

For a circular cylinder the governing parameters in the problem are: the rotational rate of the cylinder ω, its diameter $2a$, the separation between channel walls $2h$, the eccentricity of the cylinder as measured by $h_U + a - h$, and the sum of the channel lengths upstream and downstream of the cylinder L_l. In here, h_U is the upper gap, and h_L is the lower one. The governing parameters can be nondimensionalized as a Reynolds number $\mathrm{Re} = \omega (2a)^2/\nu$, where ν is the kinematic viscosity of the fluid, relative channel wall separation $s = h/a$, eccentricity $\epsilon = (h_U + a - h)/2a$, and channel length $L_l/2a$. The rotation of the cylinder, its eccentricity, and the position of the plate **B** can be varied in the experiments. Note that the average velocity in the channel is not known a priori and cannot, therefore, be used as a velocity scale. Instead we use the tangential velocity of the cylinder itself to define a Reynolds number, so that Re is not a ratio of inertial to viscous forces in the classical sense. The choice of a characteristic length to define Re is arbitrary; the other length scales in the problem are related to a via the dimensionless wall separation and eccentricity.

In the present experiments, the qualitative nature of the flow field generated by the rotating cylinder depends on the gap between the cylinder and the wall. Close to the cylinder, a primary circulation following the motion of the cylinder is always present. But on the side of the cylinder with the larger gap (normally the upper side in the present arrangement), two qualitatively different secondary flow patterns are observed. For a large h_U there is a single secondary vortex lying directly on top of the cylinder, which rotates counter to the cylinder motion. On the other hand, for a small h_U there are two small co-rotating secondary vortices located to the left and right of the cylinder. For $h_L = 0$ transition between the two patterns is observed to take place when h_U is approximately 12 mm ($s = 2.34$, $\epsilon = 0.67$). These patterns are very similar to the creeping flow eddies observed when a rotating cylinder is placed in the center of a rectangular box (Hellou and Coutanceau, 1992), or placed eccentrically within a larger circular cylinder as in journal bearings (Ottino, 1989; Ghosh et al., 1992).

From the video the time of travel of the tracer particles for a 2 cm distance in the x-direction is measured. Repeating this for different y-positions, the fluid velocity field $u^*(y)$ is determined. The first velocity measurements are made with the channel walls 14 mm apart, and with the cylinder at the lower extreme. Figure 2 shows an example of the measured velocities at four sections of the channel at different values of x, two upstream and two downstream of the cylinder. Parabolic profiles of the form $u^*(y) = U_{\max}(1 - y^2/h^2)$ are fitted to the data at each section using a least-square analysis. In general, the data at the section $x = -4$ cm fits its parabolic profile with the least error. The parabola at this section is also shown in Fig. 2. The flow at this section is almost parallel to the channel walls, while at other sections it is either affected by the inlet or outlet to the channel or is too close to the cylinder. This section is then used for the rest of the velocity measurements. We can determine an average velocity $\bar{u}^* = (1/2h)\int_{-h}^{h} u(y)dy$ at the chosen section which will also be the same at other sections. Though the integration can be done either on the experimental data using a trapezoidal rule or on the fitted parabola, we simply take $\bar{u}^* = \frac{2}{3}U_{\max}$ from now on since the difference is of the order of five percent. We can also show that the free surface of the glycerin does not affect the flow rate if it is far enough from plate **B**. The difference in average velocity in the lower channel is measured to be around one percent on changing the glycerin depth from 42.5 mm to 65 mm.

The next series of measurements are made by changing the rotation of the cylinder, but keeping the eccentricity and channel separation constant. The cylinder is again touching the bottom of the channel wall. Figure 3 shows the measured average velocity in the channel, $\bar{u}^*$, as a function of the surface speed of the cylinder, ωa. The straight line corresponds to a fit of $\bar{u}^* = 0.095\ \omega a$. The nondimensional average velocity defined by $\bar{u} \equiv \bar{u}^*/\omega a = 0.095$ under these conditions. A similar though

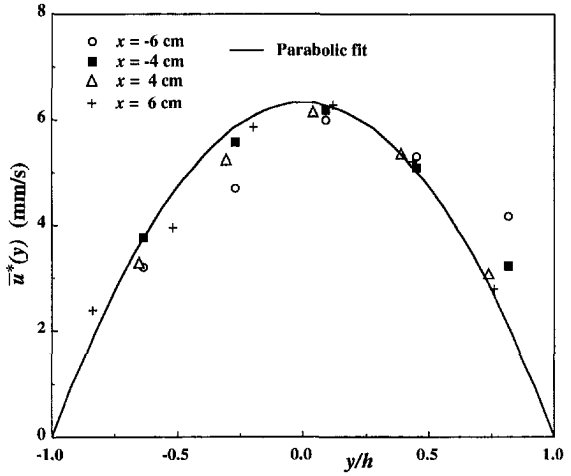

Fig. 2 Velocity profiles for Re = 1.03; s = 1.56; ϵ = 0.28. Local velocity is determined by recording the average time-of-travel of 20 tracer particles. The standard deviation for such measurements is typically ten percent of the mean.

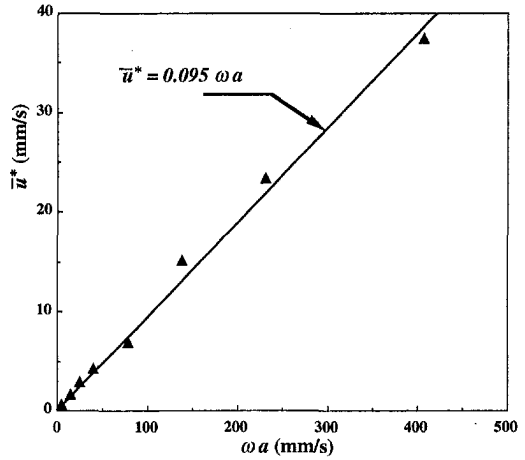

Fig. 3 Average velocity for s = 1.56; ϵ = 0.28. Uncertainty in computing the bulk velocity is ± five percent.

slightly different graph is obtained if Re, which is in the 0.1–10 range, is used as the abscissa.

Geometrical parameters like relative eccentricity and channel separation also affect the flow rate. In the present set-up we are unable to vary them independently, but can change both by moving the plate **B**. Measurements are made by changing the gap h_U and keeping Re roughly constant. Figure 4 shows the effect on the average velocity, $\bar{u}^*$, and volume flow rate per unit width, 2 $h\bar{u}^*$. Both these variables are seen to have a maximum, though at slightly different values of h_U. The maximum volume flow rate roughly corresponds to the value of h_U around which the secondary flow pattern changes from a single vortex to two.

Experiments with cylinders of square and rectangular sections are also carried out for comparison. In each case the largest dimension of the section is used to define the Reynolds number. All three cylinders have this dimension the same so that they sweep out the same area. At Re = 1.12, s = 1.78, and ϵ = 0.17, the nondimensional average fluid velocity in the channel using the circular cylinder is $\bar{u}$ = 0.046, while for the square and the rectangular cylinders it is 64.4 and 31.8 percent of this value, respectively. It appears therefore that the circular cylinder gives the best pumping performance. A weak pulsating motion superimposed on the unidirectional mean flow is observed for the two non-circular cylinders. Although not tried in here, other configurations using the same principle can be used to pump a fluid at low Reynolds numbers. For example, two counter-rotating cylinders placed symmetrically in the channel along the y-axis would perhaps be more efficient than the present asymmetric configuration. However, in a microelectromechanical systems (MEMS) application of the present idea, simplicity of construction and operation would probably be more coveted than a modest improvement in efficiency.

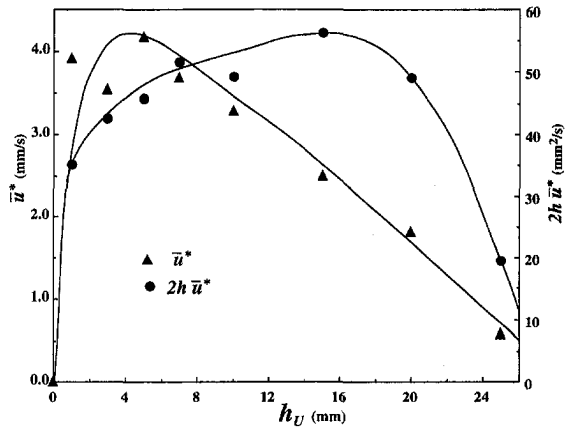

Fig. 4 Average velocity and volume flow rate for h_L = 0; Re = 1.05. Uncertainty in computing the bulk velocity is ± five percent.

The experiments reported here show that a two-dimensional, rotating cylinder eccentrically placed within a channel can drive a viscous fluid. We have been able to generate an average flow velocity that is about 10 percent of the surface speed of the cylinder. This proportionality is consistent with what can be expected for the solution of the Navier-Stokes equation in the limit of negligible inertia terms. As the Reynolds number increases, one can expect the slope of the curve in Fig. 3 to level off. It also appears that the low-Reynolds-number viscous effect is reversible in that continuous flow can rotate a cylinder placed eccentrically within channel walls.

The proposed pumping mechanism can be used at very low Reynolds numbers and is suitable for micromachine applications. Further exploration of the operation of this micropump will be numerical, as in the work by Beskok and Karniadakis (1992; 1994), and will be followed by experiments utilizing a microfabricated motor-pump assembly. The latter are obviously difficult to perform not only for the fabrication involved but also for the measurement techniques which are still under development. The proposed pumping configuration can be built using the LIGA microfabrication technique, a German-developed method based on lithography, electrodeposition and plastic molding. Our plan is to fabricate a prototype micropump in cooperation with the Center for Advanced Microstructures and Devices at Louisiana State University. The present device is also ideal for pumping high-viscosity polymers through macrochannels; while conventional pumps can potentially degrade the long-chain molecules, minimum damage would be caused by the envisioned pump.

This work is supported by National Science Foundation SGER grant no. CTS-9521612 and monitored by Drs. Robert L. Powell and Roger E. A. Arndt. We thank Dr. Alain Texier for his help with the photography and image processing.

References

Badr, H. M., Coutanceau, M., and Dennis, S. C. R., 1990, "Unsteady Flow Past a Rotating Circular Cylinder at Reynolds Numbers 103 and 104," *Journal of Fluid Mechanics,* Vol. 220, pp. 459–484.

Badr, H. M., Dennis, S. C. R., and Young, P. J. S., 1989, "Steady and Unsteady Flow Past a Rotating Circular Cylinder at Low Reynolds Numbers," *Computers and Fluids,* Vol. 17, pp. 579–609.

Bart, S. F., Tavrow, L. S., Mehregany, M., and Lang, J. H., 1990, "Microfabricated Electrohydrodynamic Pumps," *Sensors and Actuators A,* Vol. 21–23, pp. 193–197.

Beskok, A., and Karniadakis, G. E., 1992, "Simulation of Slip-Flows in Complex Micro-Geometries," *Micromechanical Systems,* D. Cho, J. P. Peterson, A. P. Pisano and C. Friedrich, eds., ASME DSC-Vol. 40, pp. 355–370.

Beskok, A., and Karniadakis, G. E., 1994, "Simulation of Heat and Momentum Transfer in Complex Micro-Geometries," *Journal of Thermophysics and Heat Transfer,* Vol. 8, pp. 647–655.

Esashi, M., Shoji, S., and Nakano, A., 1989, "Normally Closed Microvalve Fabricated on a Silicon Wafer," *Sensors and Actuators,* Vol. 20, pp. 163–169.

Fuhr, G., Hagedorn, R., Müller, T., Benecke, W., and Wagner, B., 1992, "Microfabricated Electrohydrodynamic (EHD) Pumps for Liquids of Higher Conductivity," *Journal of Microelectromechanical Systems,* Vol. 1, pp. 141–145.

Ghosh, S., Chang, H.-C., and Sen, M., 1992, "Heat-Transfer Enhancement due to Slender Recirculation and Chaotic Transport between Counter-Rotating Eccentric Cylinders," *Journal of Fluid Mechanics,* Vol. 238, pp. 119–154.

Hellou, M., and Coutanceau, M., 1992, "Cellular Stokes Flow Induced by Rotation of a Cylinder in a Closed Channel," *Journal of Fluid Mechanics,* Vol. 236, pp. 557–577.

Ingham, D. B., and Tang, T., 1990, "A Numerical Investigation into the Steady Flow Past a Rotating Circular Cylinder at Low and Intermediate Reynolds Numbers," *Journal of Computational Physics,* Vol. 87, pp. 91–107.

Kimura, T., Tsutahara, M., and Wang, Z.-Y., 1992, "Wake of a Rotating Circular Cylinder," *AIAA Journal,* Vol. 30, pp. 555–556.

Lipkin, R., 1993, "Micro Steam Engine Makes Forceful Debut," *Science News,* Vol. 144, Sept., p. 197.

Moroney, R. M., White, R. M., and Howe, R. T., 1991, "Ultrasonically Induced Microtransport," *Proceedings IEEE MEMS 91* (Nara, Japan), IEEE, New York, pp. 277–282.

O'Connor, L., 1992, "MEMS: Micromechanical Systems," *Mechanical Engineering,* Vol. 114, Feb., pp. 40–47.

Odell, G. M., and Kovasznay, L. S. G., 1971, "A New Type of Water Channel with Density Stratification," *Journal of Fluid Mechanics,* Vol. 50, pp. 535–543.

Ohba, H., and Kuroda, S., 1993, "Numerical Analysis of Flows around a Rotating Square Cylinder," *JSME International Journal, Series B,* Vol. 36, pp. 592–597.

Ottino, J. M., 1989, *The Kinematics of Mixing: Stretching, Chaos, and Transport,* Cambridge University Press, U.K.

Richter, A., Plettner, A., Hofmann, K. A., and Sandmaier, H., 1991, "A Micromachined Electrohydrodynamic (EHD) Pump," *Sensors and Actuators A,* Vol. 29, pp. 159–168.

Smits, J. G., 1990, "Piezoelectric Micropump with Three Valves Working Peristaltically," *Sensors and Actuators A,* Vol. 21–23, pp. 203–206.

Tang, T., and Ingham, D. B., 1991, "On the Steady Flow Past a Rotating Circular Cylinder at Reynolds Numbers 60 and 100," *Computers and Fluids,* Vol. 19, pp. 217–230.

Taylor, Sir G., 1972, "Low-Reynolds-Number Flows," *Illustrated Experiments in Fluid Mechanics,* National Committee for Fluid Mechanics Films, M.I.T. Press, Cambridge, MA, pp. 47–54.

Van Lintel, H. T. G., Van de Pol, F. C. M., and Bouwstra, S., 1988, "A Piezoelectric Micropump Based on Micromachining of Silicon," *Sensors and Actuators,* Vol. 15, pp. 153–167.

Zaki, T. G., Sen, M., and Gad-el-Hak, M., 1994, "Numerical and Experimental Investigation of Flow Past a Freely Rotatable Square Cylinder," *Journal of Fluid Mechanics,* Vol. 8, pp. 555–582.